

# Development status of superconducting solenoid for the MuHFS experiment at the J-PARC

**Ken-ichi Sasaki, Michinaka Sugano, Hiromi Iinuma, Toru Ogitsu,  
Naohito Saito, Koichiro Shimomura and Akira Yamamoto**

KEK, 1-1, Oho, Tsukuba, Ibaraki, 305-0801, JAPAN

E-mail: [ken-ichi.sasaki@kek.jp](mailto:ken-ichi.sasaki@kek.jp)

**Abstract.** The development of a superconducting solenoid for a new Muonium HyperFine Structure, MuHFS, measurement at J-PARC has been underway since 2010. High homogeneity of magnetic field below 1 ppm is required for this experiment. Superconducting main coils were designed and error fields caused by the main coil misalignment were evaluated for designing superconducting shim coils. The coil deformation by the coil winding, thermal contraction and hoop stress due to the magnetic force was also estimated. A quench protection study was performed to determine the required parameters of the superconducting strand.

## 1. Introduction

A new measurement of hyperfine transitions in the ground state of muonium, called the HFS experiment, is part of the new J-PARC project [1]. The goal of this experiment is to measure the value of the ground state hyperfine structure interval of muonium down to the level of a few ppb, and also determine the ratio of muon and proton magnetic moment with accuracy of a 10 ppb. For this experiment, a superconducting solenoid system with a magnetic field of 3.4 T is under development [2]. The solenoid requires a high field uniformity with a deviation less than 1 ppm within the spheroid region of 20 cm in diameter and 30 cm in length. This magnet is also considered as a prototype magnet for the g-2/EDM experiment at J-PARC [3], in order to minimize the development time and maximize the synergy between both experiments.

This paper reports the current status of the HFS magnet system development. The development of a field monitoring system to evaluate the field uniformity are also discussed.

## 2. Magnet design

### 2.1. Overview

A schematic view of the magnet system for the MuHFS experiment is shown in Figure 1. A NbTi superconductor will be used for the coil to minimize the cost of the strand. The strand diameter and Cu/Sc ratio are 2.0 mm and 6, respectively. The coil is immersed in a liquid helium of 4.2 K, and the re-condensation cryocoolers will be used for long term operation. The magnet will be operated in the persistent current mode to minimize the field fluctuation due to the ripples of the power supply.

### 2.2. Main coil design

Figure 2 shows the ideal coil block geometry of the MuHFS magnet. The magnet consists of 6 main coils and 2 shielding coils. The inner and outer diameter of the magnet are about 600 mm and 1460 mm, respectively. Contour lines in Figure 2 represent the field difference of  $\pm 0.5$  ppm from the center field of about 3.4 T at the current density of  $1.18 \times 10^8$  A/m<sup>2</sup>, corresponding to the strand current of about 411 A. The required uniform region is also plotted in Figure 2 by the dotted line. The Figure indicates that this coil configuration satisfies the required uniformity. The peak field on the coil and the stored energy are about 4.7 T and 4.0 MJ, respectively.

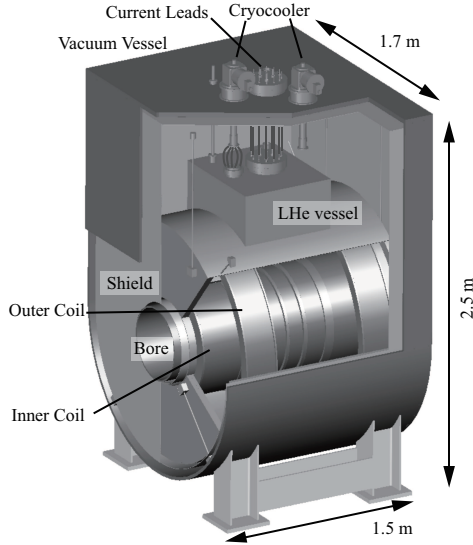


**Figure 1.** Schematic view of the magnet system for the HFS experiment at J-PARC.

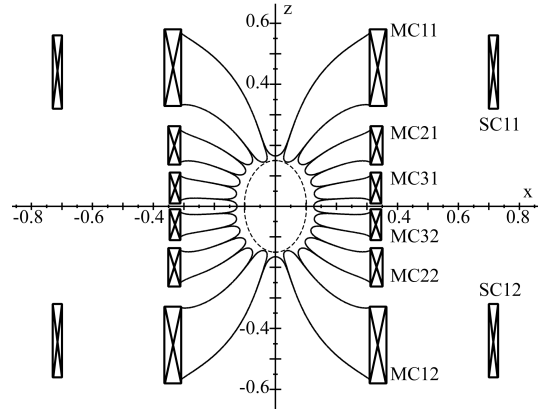


**Figure 2.** Coil cross sections and calculated field distribution. The contour lines represent the field difference of  $\pm 0.5$  ppm from the field at the magnet center. The dotted line represents the required uniform region.

### 2.3. Quench Protection

The quench protection performance of this coil was simulated. Fig. 3 shows the electrical circuit for the quench protection study in the case of persistent current operation mode. All the coils including the shield coils and the persistent current switch, PCS, are connected in series. The diodes have a forward voltage of 5 V and are connected in parallel with each section as shown in Fig. 3. It is assumed in the simulation that the coils are adiabatic, and that the normal zone does not propagate between coils.

Fig. 4 shows the simulation result during the quench of the MC31 coil. The current decay in the circuit including the quenched coil, is almost completed in about 15 sec after the quench, while the current in the another circuit is only slightly decreased. This is caused by the mutual inductance coupling with the active shield coils, which are wound in the counter direction to the main coils. A quench in the MC31 is the most serious case in terms of the peak temperature of the superconductor. However, the peak temperature after a quench of about 230 K is acceptable. The highest resistive voltage generates in the case of the quench in the SC11 coil. Even in that case, the peak voltage in the coil is allowable, about 2.1 kV. These results indicate that the magnet could be protected without any active protection scheme, such as protection heaters.

### 2.4. Field Tuning Scheme

In order to achieve a sufficiently high homogeneity of the magnetic field, with deviations below 1 ppm, various sources of error field have to be considered beforehand, and the correction

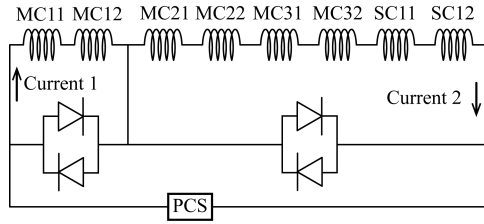


**Figure 3.** Electrical circuit for the study of quench protection during persistent current operation.

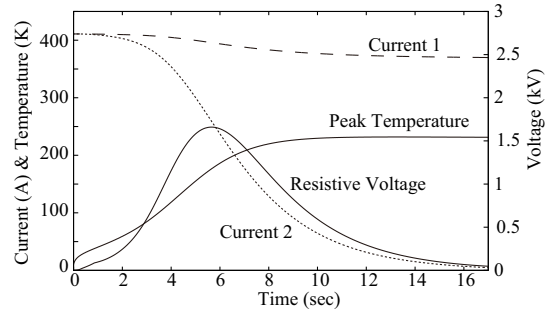


**Figure 4.** Quench simulation result in the case of the MC31 quench.

scheme must be determined ahead of time as much as possible. The error field due to the coil misalignments were evaluated. We find the error field is less than about 190 ppm, even if the errors in magnet construction were as large as 0.1 mm and 0.1 mrad [2], In order to guard against such a huge error field in the HFS magnet, a combination of steel pieces and superconducting shim coils will be employed; such a method is commonly used in commercial MRI magnets [4]. The error field would be roughly compensated to several ppm by steel pieces mounted on the surface of the magnet bore. For example, when the steel ring with 0.42 m in inner diameter and rectangular cross section ( $10 \times 20$  mm) is inserted in the bore of the coil MC31, the field change at the magnet center is calculated to be about 521 ppm. The complicated error field distribution could be corrected by arranging positions of steel pieces. The detailed design work of the superconducting shim coil is ongoing.

### 3. Field Monitoring System

#### 3.1. Moving Stage

In order to compensate the error field with the scheme mentioned in the previous Section, a precise field monitoring system is required. An NMR probe will be used to measure the magnetic field; however, the probe size is very small, less than 5 mm. Therefore, a 3-axis moving stage is required. Figure 5 shows the schematic view of the  $r$ - $\theta$ - $z$  moving stage developed now. The NMR probe is mounted on the slide stage in radial direction, and the slide stage is mounted on a rotating disk. Both the radial slide stage and the rotating disk are driven by ultrasonic motors. The whole stage can move along the  $z$ -axis on the rail, and is driven by a stepping motor, which is 2 m away from the magnet end, far away enough so that there will be no significant distortion of the magnetic field. Almost all the parts of this system consist of non-metallic material except for the case of the ultrasonic motor and NMR probe, which are made by aluminum and copper.

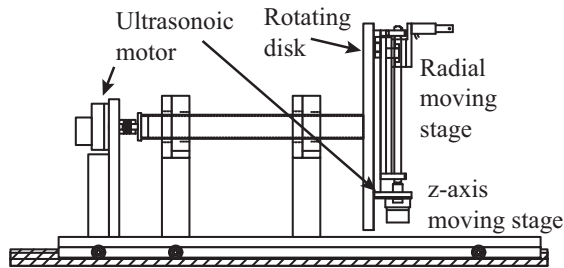
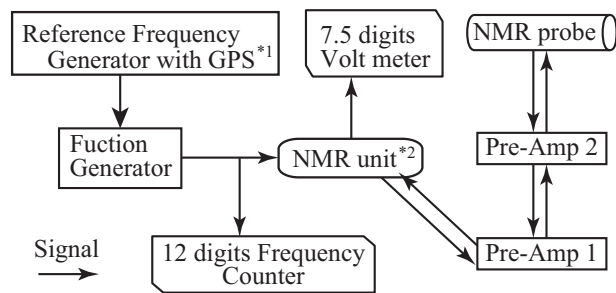


**Figure 5.** Schematic view of the  $r$ - $\theta$ - $z$  moving stage.



\*1: EFM-3000AXK (Echo-Denshi); \*2: SecureSync (SPECTRACOM)

**Figure 6.** Connection diagram of the NMR system.

### 3.2. NMR system

Figure 6 shows the connection diagram of the field measurement system. A Continuous Wave type (CW) NMR unit and probe are used for this system. The most effective way to improve the stability and accuracy of the CW-NMR system is to improve the accuracy of the RF signal input to the NMR sample. In our system, a reference frequency generator with GPS, which has an accuracy of  $1 \times 10^{-12}$ , is connected to the function generator. The NMR unit output is a voltage proportional to the measured field.

The stability of this NMR system was checked using 3 T MRI magnet at the NIRS, National Institute of Radiological Sciences. Figure 7(a) shows the error distribution of the RF frequency output from the function generator measured by the frequency counter. The input frequency is 12.771271699 MHz, corresponding to a field strength of 2.9996145 T. The standard deviation is measured to be  $1.4 \times 10^{-4}$  ppm. This demonstrates that the output signal of the function generator is highly stabilized thanks to the reference frequency generator, compared to the required accuracy of 1 ppm. However, the output voltage of the NMR unit was not sufficiently stable. Figure 7(b) shows the error distribution of the output voltage of the NMR unit, and the standard deviation is 0.025 ppm. The horizontal axis is the voltage difference between the mean value of the measured voltage. The reason for this result is not clear. However, one suspected source is the pre-amps between NMR probe and unit. In this test system, the frequency of the RF signal is amplified by ten times in the pre-amp circuits. This modulation seems to decrease the stability. A new NMR unit and pre-amps excluding the frequency modulation circuit will be tested in the next round of tests.

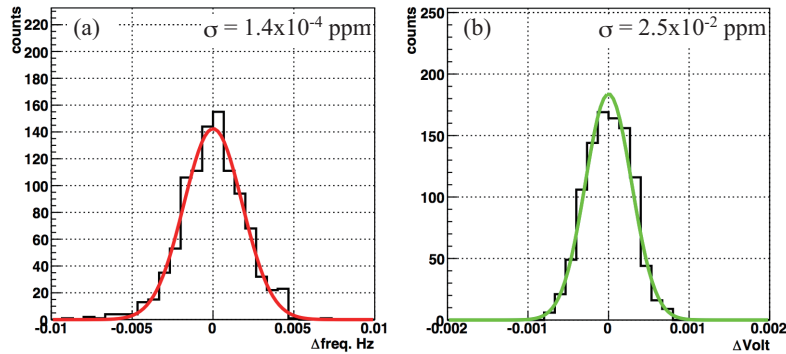


**Figure 7.** Error field distribution of the NMR system. (a): Frequency of the output signal of the function generator. (b): Output voltage of the NMR unit.

## 4. Summary

A superconducting solenoid with high field homogeneity for the muonium HFS experiment is being developed. The design of superconducting main coils was completed. The quench protection study showed that the main coils could be safely protected during the magnet quench. The field tuning scheme was discussed and both the steel pieces and the superconducting shim coils were considered. The field monitoring system using the continuous wave type NMR system was tested, and the new system will be tested at the NIRS. The basic design work will be finished soon, and the magnet system including the field monitoring system will be ready for the experiment in mid-2014.

## References

- [1] Shimomura K 2011 these proceedings
- [2] Sasaki K, Sugano M, Ohkubo R, Inuma H, Ogitsu T, Saito N, Shimomura K and Yamamoto A 2011 *22nd Int. Conf. on Magnet Technology*
- [3] Saito N 2011 these proceedings
- [4] Robitaille P M and Berliner L 2006 *Ultra High Field Magnetic Resonance Imaging* (New York: Springer-Verlag)